Pergamon

Int. J. Heat Mass Transfer. Vol. 38, No. 1, pp. 39–45, 1995

0017-9310/95 $9.50 + 0.00

0017-9310(94)00146-4

An inverse analysis for estimating the time-varying inlet temperature in laminar flow inside a parallel plate duct

J. C. BOKAR and M. N. ÖZISIK†

Mechanical and Aerospace Engineering Department, North Carolina State University, Raleigh, NC 27695-7910, U.S.A.

(*Received* 10 *January* 1994 *and in final form* 13 *May* 1994)

Abstract—An inverse problem utilizing the conjugate gradient method of minimization with adjoint problem is used to estimate the timewise variation of the inlet temperature of a thermally developing, hydrodynamically developed laminar flow between parallel plates by utilizing transient temperature measurements from a single thermocouple located downstream of the entrance. It is assumed that there is no prior information available on the functional form of time dependence of the inlet temperature other than that which can be inferred from the measured downstream temperatures. The effects of functional form of the inlet temperature, sensor position, magnitude of measurement error and data sampling rate on the accuracy of estimates are examined. In order to examine the accuracy of the method under most strict conditions, timewise variations in the form of step changes were also studied. The inverse analysis considered here could predict the timewise variation of inlet temperature even under such strict conditions. The estimates are notably more accurate when the thermocouple is placed near the entrance.

1. INTRODUCTION

Estimating the time-varying inlet condition for forced convective flow in ducts can be of great interest to the engineer. Often, one may not know the actual inlet condition or not be able to measure it directly at the inlet of the duct, yet this may be of utmost importance in controlling the operation of a process upstream. Only a small amount of work is available in the area of inverse analysis of estimating the unknown inlet temperature of flow inside ducts. The steady-state problems of estimating spatially varying wall heat flux is considered in ref. [1], the estimation of the inlet condition for steady flow in a duct in ref. [2], and the estimation of spatially varying wall temperature and heat flux for free convective flows in ref. [3]. In the transient problem considered here, only one thermocouple located at the centerline is used, and many time measurements, varying from 100 to 200 readings, are taken. Tests were also conducted by varying the location of the thermocouple.

In this work the conjugate gradient method of minimization with adjoint problem is used to estimate the inlet temperature by utilizing simulated measured temperatures at some downstream location without any prior information on the functional form of the inlet condition.

2. ANALYSIS

The inverse analysis of function estimation presented here utilizes the conjugate gradient method of minimization which requires the solution of the *direct problem*, the *sensitivity problem* and the *adjoint problem* as discussed in refs. [4, 5]. The direct problem is a well-posed problem when the inlet temperature distribution function, $F(\tau)$ is known; however, when $F(\tau)$ is unknown and to be determined from the measurements taken at some downstream location inside the duct at various times, the problem becomes an inverse problem which is ill-posed. Each of these three distinct problems are described below before presenting the general algorithm to solve the inverse problem.

2.1. *Direct problem*

Consider laminar forced convection inside a parallel plate duct with the walls and the fluid at a constant uniform prescribed temperature. At time $\tau = 0$, the inlet temperature, $\Theta(0, R, \tau)$ begins to vary as a function of time in the form, $F(\tau)$. Figure 1 describes the geometry and coordinates.

The velocity profile is given in the dimensionless form as

$$U(R) = \tfrac{3}{2}(1 - R^2). \tag{1}$$

Neglecting axial conduction and free convection in the flow, the energy equation is written as

$$\frac{\partial \Theta(Z, R, \tau)}{\partial \tau} + U(R)\frac{\partial \Theta(Z, R, \tau)}{\partial Z} = \frac{\partial^2 \Theta(Z, R, \tau)}{\partial R^2} \tag{2a}$$

† Author to whom correspondence should be addressed.

NOMENCLATURE

F^k	current estimate of inlet temperature
$F(\tau)$	$[f(t)-T_i]/T_i$, dimensionless inlet temperature
$f(t)$	functional form of inlet temperature variation
$J(F)$	functional, defined by equation (3)
$J'(\tau)$	gradient of functional
L	channel half-width
P^k	direction of descent at the kth iteration defined by equation (11)
R	y/L, dimensionless normal coordinate
R^*	measurement location in R-direction
t	time
T_i	initial temperature
$U(R)$	$\frac{3}{2}(1-R^2)$, dimensionless velocity
$u(y)$	$\frac{3}{2}u_m(1-(y/L)^2)$, velocity
u_m	$(-L^2/2\mu)\mathrm{d}P/\mathrm{d}x$
x	axial coordinate in flow direction
y	normal coordinate
Y	dimensionless measured temperature
Z	$\alpha x/u_m L^2$, dimensionless flow direction coordinate
Z^*	measurement location in Z-direction.

Greek symbols

α	thermal diffusivity
β^k	step size defined by equation (14)
$\Delta\Theta$	sensitivity function defined by problem (4)
δ	Dirac-delta function
ε	convergence criteria
γ^k	conjugate coefficient at the kth iteration defined by equation (10)
$\lambda(\tau, R, Z)$	adjoint function defined by problem (6)
Θ	$[T(x,y,t)-T_i]/T_i$, dimensionless temperature
σ	standard deviation of measurement
τ	$\alpha t/L^2$, dimensionless time
ω	random variable.

Superscripts

k	number of iteration
*	measurement location.

Subscripts

f	total extent of variable (i.e. τ_f or Z_f)
m	mean value.

for $0 < R < 1, Z > 0, \tau > 0$. The associated boundary conditions are taken as

$$\frac{\partial\Theta(Z,0,\tau)}{\partial R} = 0 \quad \text{at } R=0 \quad Z>0 \quad \tau>0 \tag{2b}$$

$$\Theta(Z,1,\tau) = 0 \quad \text{at } R=1 \quad Z>0 \quad \tau>0 \tag{2c}$$

$$\Theta(0,R,\tau) = F(\tau) \quad \text{at } Z=0 \quad 0 \leqslant R < 1 \quad \tau>0 \tag{2d}$$

and the initial condition as

$$\Theta(Z,R,0) = 0 \quad \text{at } \tau=0 \quad 0<R<1 \quad Z \geqslant 0 \tag{2e}$$

where various dimensionless terms are defined as

$$\Theta = \frac{T(x,y,t)-T_i}{T_i} \qquad \tau = \frac{\alpha t}{L^2}$$

$$R = \frac{y}{L} \qquad Z = \frac{\alpha x}{u_m L^2}$$

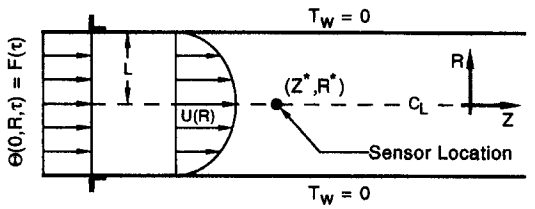

Fig. 1. Geometry and coordinates.

$$U(R) = \frac{u(y)}{u_m} \qquad F(\tau) = \frac{f(t)-T_i}{T_i}.$$

Here α is the thermal diffusivity of the fluid, u_m is the mean velocity and T_i is the initial temperature. The direct problem, defined by equation (2), will be solved by finite differences, using an implicit upwind scheme.

2.2. *Sensitivity problem*

When the inlet condition $F(\tau)$ is unknown, problem (2) becomes an inverse problem, and its solution can be recast as a problem of optimal control, i.e. choose the control function, $F(\tau)$, which minimizes the following functional, J:

$$J[F(\tau)] = \int_0^{\tau_f} [\Theta(Z^*, R^*, \tau; F(\tau)) - Y(Z^*, R^*, \tau)]^2 \,\mathrm{d}\tau \tag{3}$$

where $\Theta(Z^*, R^*, \tau; F(\tau))$ is the estimated temperature at the measurement location $[R^*, Z^*]$, based on the current estimation of the inlet temperature, $F(\tau)$, while $Y(Z^*, R^*, \tau)$ is the measured temperature at the same location. Let us now assume that $F(\tau)$ changes by an increment ΔF, and as a result the temperature, Θ, also changes by the amount $\Delta\Theta$. We now substitute $\Theta + \Delta\Theta$ and $F + \Delta F$ into the original problem defined

by equation (2), and subtract from the resulting system those given by equation (2) to produce the following sensitivity problem:

$$\frac{\partial \Delta\Theta(Z,R,\tau)}{\partial \tau}+U(R)\frac{\partial \Delta\Theta(Z,R,\tau)}{\partial Z}=\frac{\partial^2 \Delta\Theta(Z,R,\tau)}{\partial R^2} \tag{4a}$$

in $0<R<1, Z>0, \tau>0$, with

$$\frac{\partial \Delta\Theta(Z,0,\tau)}{\partial R}=0 \quad \text{at } R=0 \quad Z>0 \quad \tau>0 \tag{4b}$$

$$\Delta\Theta(Z,1,\tau)=0 \quad \text{at } R=1 \quad Z>0 \quad \tau>0 \tag{4c}$$

$$\Delta\Theta(0,R,\tau)=\Delta F(\tau) \quad \text{at } Z=0 \quad 0<R<1 \quad \tau>0 \tag{4d}$$

and

$$\Delta\Theta(Z,R,0)=0 \quad \text{at } \tau=0 \quad 0<R<1 \quad Z\geqslant 0. \tag{4e}$$

The sensitivity problem defined by equation (4) will be solved by the same method as that used for the solution of the direct problem described previously.

2.3. *Adjoint problem*

The adjoint problem is obtained by multiplying equation (2a) by the adjoint function $\lambda(\tau,Z,R)$, integrating the resulting expression over the time and space domain and adding the result to the functional given by equation (3). Hence,

$$J[F(\tau)]=\int_{\tau=0}^{\tau_f}[\Theta(Z^*,R^*,\tau;F(\tau))-Y(Z^*,R^*,\tau)]^2\,d\tau+\int_{\tau=0}^{\tau_f}\int_{Z=0}^{Z_f}\int_{R=0}^{1}\lambda(\tau,Z,R)\times\left[\frac{\partial\Theta}{\partial\tau}+U(R)\frac{\partial\Theta}{\partial Z}-\frac{\partial^2\Theta}{\partial R^2}\right]dR\,dZ\,d\tau. \tag{5}$$

Note that, when $\Theta(Z,R,\tau)$ is the exact solution of problem (2), the last term on the right hand side of equation (5) vanishes and the original functional (3) is recovered.

We now perturb $F(\tau)$ by $\Delta F(\tau)$ and Θ by $\Delta\Theta$ in equation (5), and subtract equation (5) from the resulting expression to get the variation, ΔJ, of the functional J. By employing integration by parts and utilizing the boundary conditions from the sensitivity problem and also requiring that the coefficients of $\Delta\Theta$ in the resulting equation should vanish, the following adjoint problem is generated:

$$2[\Theta(Z,R,\tau)-Y(Z,R,\tau)]\delta(Z-Z^*)\delta(R-R^*)-\frac{\partial\lambda(\tau,Z,R)}{\partial\tau}-U(R)\frac{\partial\lambda(\tau,Z,R)}{\partial Z}-\frac{\partial^2\lambda(\tau,Z,R)}{\partial R^2}=0 \tag{6a}$$

where $\delta(\ )$ is the Dirac-delta function. The boundary conditions become

$$\frac{\partial\lambda(\tau,Z,0)}{\partial R}=0 \quad \text{at } R=0 \quad Z>0 \quad \tau>0$$

$$\lambda(\tau,Z,1)=0 \quad \text{at } R=1 \quad Z>0 \quad \tau>0$$

$$\lambda(\tau,Z_f,R)=0 \quad \text{at } Z=Z_f \quad 0<R<1 \quad \tau>0 \tag{6b}$$

and the final time condition at $\tau=\tau_f$ is given by

$$\lambda(\tau_f,Z,R)=0 \quad \text{at } \tau=\tau_f \quad 0<R<1 \quad Z\geqslant 0. \tag{6c}$$

Then the following integral term is left:

$$\Delta J[F(\tau)]=-\int_{\tau=0}^{\tau_f}\Delta F(\tau)\times\left[\int_{R=0}^{1}\lambda(\tau,0,R)U(R)\,dR\right]d\tau. \tag{7}$$

When the function is considered to be square integrable, the following relation holds [4]:

$$\Delta J[F(\tau)]=\int_{\tau=0}^{\tau_f}J'(\tau)\Delta F(\tau)\,d\tau. \tag{8}$$

A comparison of equations (7) and (8) reveals that the gradient of the functional, $J'(\tau)$, is

$$J'(\tau)=-\int_{R=0}^{1}\lambda(\tau,0,R)U(R)\,dR. \tag{9}$$

The adjoint problem is different from the direct problem in that the current estimate, $\Theta(Z,R,\tau)$, minus measured temperature, $Y(Z,R,\tau)$, is a source term in equation (6a). Also, the final time condition, τ_f, and final space condition, Z_f, are specified instead of a usual initial and inlet condition. However, with the replacement of the time variable by $\bar{\tau}=\tau_f-\tau$ and the space variable by $\bar{Z}=Z_f-Z$, a standard type problem can be produced which can be solved by using the finite difference approach referred to previously.

2.4. *The conjugate gradient method of minimization*

The following iterative procedure is suggested [5] for the inverse problem, assuming that the functions $\Theta(Z,R,\tau)$, $\Delta\Theta(Z,R,\tau)$, $\lambda(\tau,Z,R)$ and $J'(\tau)$ are available at the kth iteration:

$$F^{k+1}=F^k-\beta^k P^k \quad k=0,1,2,\ldots \tag{10}$$

where $P^k\equiv P^k[F(\tau)]$ is the direction of descent determined from the combination of the gradient at the kth step, and the descent direction at the $(k-1)$th step in the form

$$P^k=(J')^k+\gamma^k P^{k-1}. \tag{11}$$

Here, γ^k is the conjugate coefficient and is computed from the expression

$$\gamma^k=\frac{\int_{\tau=0}^{\tau_f}[J'^k(\tau)]^2\,d\tau}{\int_{\tau=0}^{\tau_f}[J'^{k-1}(\tau)]^2\,d\tau} \quad \text{with } \gamma^0=0. \tag{12}$$

The coefficient β^k, which determines the step size in going from F^k to F^{k+1}, is computed by minimizing $J(F^{k+1})$ with respect to β^k, i.e.

$$\min_{\beta} J(F^{k+1}) = \min_{\beta} \int_{\tau=0}^{\tau_f} [\Theta(F^k - \beta^k P^k) - Y]^2 \, d\tau \tag{13}$$

which produces

$$\beta^k = \frac{\int_{\tau=0}^{\tau_f} \Delta\Theta(P^k)[\Theta(F^k) - Y] \, d\tau}{\int_{\tau=0}^{\tau_f} [\Delta\Theta(P^k)]^2 \, d\tau}. \tag{14}$$

2.5. *The stopping criterion*

In all practical experimental situations it is expected that some error will be introduced into the measurements. The discrepancy principal [6] is used to terminate the iteration process suggested by equation (10). Assuming that $\Theta(Z^*, R^*, \tau) - Y(Z^*, R^*, \tau) \cong \sigma$, where σ is the standard deviation of measurements, has a constant value for all measurements, we substitute this result into equation (3) to obtain

$$J = \int_{\tau=0}^{\tau_f} \sigma^2 \, d\tau = \sigma^2 \tau_f \equiv \varepsilon^2 \tag{15}$$

where ε^2 is the desired stopping criterion. The iterations are stopped when $J < \varepsilon^2$.

2.6. *The computational algorithm*

The computational procedure for this inverse problem can be summarized in the following algorithm:

Assuming that an estimate of $F(\tau)$ is available at the kth iteration,

Step 1—solve the direct problem given by equation (2), and compute the temperature at the measurement location $[Z^*, R^*]$,

Step 2—knowing $\Theta(Z^*, R^*, \tau)$ and the measured temperatures, $Y(Z^*, R^*, \tau)$, compute the adjoint function $\lambda(\tau, 0, R)$ from the solution of the adjoint problem given by equation (6),

Step 3—given $\lambda(\tau, 0, R)$, calculate J' from equation (9),

Step 4—compute the conjugate coefficient, γ^k, from equation (12),

Step 5—calculate the direction of descent, P^k, from equation (11),

Step 6—setting $P^k = \Delta F(\tau)$, solve the sensitivity problem given by equation (4), for $\Delta\Theta$,

Step 7—compute the step size, β^k, from equation (14),

Step 8—compute $F^{k+1}(\tau)$ from equation (10),

Step 9—check if the stopping criterion is met; if not, return to Step 1.

3. RESULTS AND DISCUSSION

To illustrate the accuracy of the inverse algorithm in predicting $F(\tau)$, we examine three functional test cases; a triangular ramp, a double step, and a sine curve, as illustrated in Fig. 2. The first two represent very difficult functions to predict due to the discontinuities present in the function. As the sine curve is smooth and continuous, its estimation should not pose difficulty. Over the total experiment time of 3.6×10^{-3} in dimensionless terms, 200 equal time steps are considered, corresponding to a sampling frequency of 1.8×10^{-5}. The total dimensionless length of the duct, taken as 8.2×10^{-3}, with 60 equal divisions corresponding to $\Delta Z = 1.367 \times 10^{-4}$, was long enough for all test locations to lay in the thermally developing region. A representative total time and total length in dimensional terms are $t_f = 30$ s, and $x_f = 1.64$ m for air with a mean velocity of 2.4 cm s^{-1} in a duct with half width $L = 0.5$ m. The sensors are placed on the centerline ($R^* = 0$) of the duct at downstream locations, $Z^* = 5\Delta Z$ and $20\Delta Z$. The centerline was chosen for all measurements in order to minimize the effects of the wall temperature on the reading of the sensor at the measurement location.

The simulated measured experimental temperature data, Y_{measured}, are generated by adding an error term, $\omega\sigma$, to the exact temperature Θ_{exact} obtained from the solution of the direct problem (2) as

$$Y_{\text{measured}} = \Theta_{\text{exact}} + \omega\sigma \tag{16}$$

where σ is the selected standard deviation for the measured data. The random variable ω is calculated by the IMSL subroutine DRNNOR [7] and chosen to lie in the range of $-2.576 < \omega < 2.576$ which represents a 99% confidence bound for the measured temperature.

Test case 1: *triangular ramping function*

The time-dependent inlet condition for a triangular ramp function illustrated in Fig. 2a is assumed to vary in the form

$$F(\tau) = \begin{cases} 1111.11\tau & \text{for } 0 < \tau \leqslant 9.2 \times 10^{-4} \\ -833.33(\tau - 9 \times 10^{-4}) + 1 & \\ \quad \text{for } 9.2 \times 10^{-4} < \tau \leqslant 1.51 \times 10^{-3} & \\ 0.5 \quad \text{for } 1.51 \times 10^{-3} < \tau \leqslant \tau_f. & \end{cases} \tag{17}$$

Figure 3 shows typical measured temperatures at two different downstream locations for $\sigma = 0.01$, which correspond to approx. 3% measured error based on the maximum measured temperature. These curves show that the steady measured value is achieved after a certain time period. The inverse problem is based on all data taken before the steady temperature has been reached, since the measured data taken after

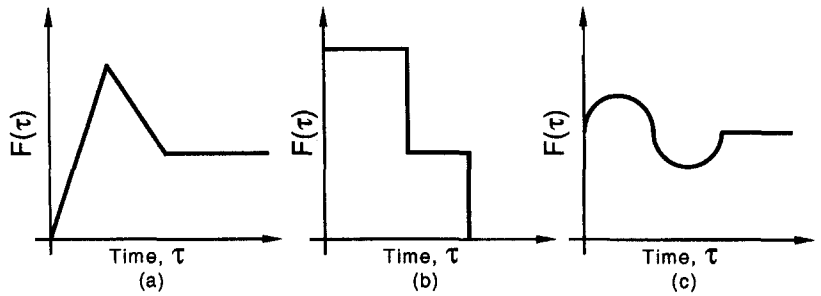

Fig. 2. Three test cases considered for the inlet temperature functions to examine the accuracy of inverse analysis: (a) triangular ramp; (b) double step; and (c) sine curve.

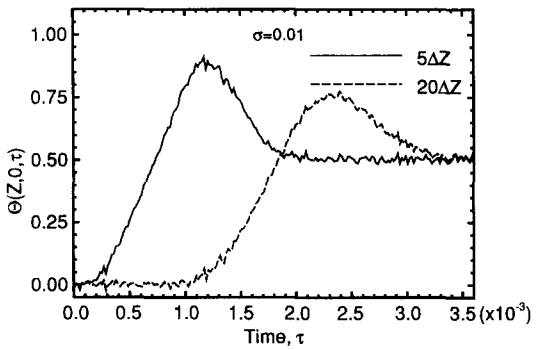

Fig. 3. Simulated measured temperatures at downstream locations $5\Delta Z$ and $20\Delta Z$ for triangular ramp pulse, with $\sigma = 0.01$.

the establishment of the steady state contribute no additional information. Under actual measurement conditions, this reasoning would most likely be used to determine the stopping time of the experiment. Also, we chose the steady value of the measured temperature as the initial guess for the computational algorithm. This choice alleviates one of the difficulties associated with the conjugate gradient method, that is, the final time value of the estimation is the same as the initial guess [1].

Figure 4 illustrates the effects of the standard deviations $\sigma = 0.01$ and $\sigma = 0.03$, on the accuracy of the estimates by inverse analysis. Here the solid lines represent the exact solution. These standard deviations represent 3% and 10% measurement error based on the maximum temperature. It is clear that, as error increases, the accuracy of the prediction decreases; however, even the $\sigma = 0.03$ estimate is quite good. Figure 5 shows the effects of measurement location on the accuracy of the estimation. The $5\Delta Z$ location, which is close to the entrance, produces more accurate results, as expected. The $20\Delta Z$ location shows a marked decrease in accuracy, particularly near the discontinuity in slope, with the estimate oscillating around the exact function elsewhere.

Test case 2: double step function

The inlet condition for a double step function illustrated in Fig. 2b is assumed in the form

$$F(\tau) = \begin{cases} 1 & \text{for } 0 < \tau \leqslant 8.2 \times 10^{-4} \\ 0.5 & \text{for } 8.2 \times 10^{-4} < \tau \leqslant 1.22 \times 10^{-3} \\ 0 & \text{for } 1.22 \times 10^{-3} < \tau \leqslant \tau_f \end{cases} \quad (18)$$

which represents a very strict test for the inverse analysis. Figure 6 shows typical measured temperatures at $Z = 5\Delta Z$ and $20\Delta Z$ downstream locations for $\sigma = 0.01$, while Fig. 7 compares the results of the inverse solutions at $Z = 5\Delta Z$ and $20\Delta Z$ downstream

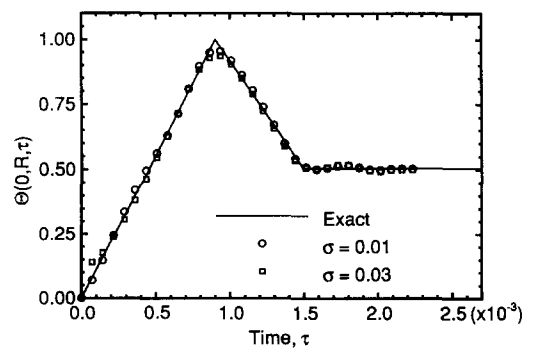

Fig. 4. The effects of standard deviation for $\sigma = 0.01$ and $\sigma = 0.03$ on the accuracy of the estimate for triangular ramp pulse at downstream location $5\Delta Z$.

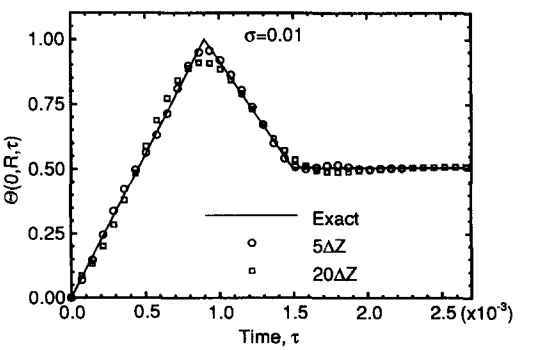

Fig. 5. The effects of sensor locations $5\Delta Z$ and $20\Delta Z$ on the accuracy of the estimate for triangular ramp pulse, with $\sigma = 0.01$.

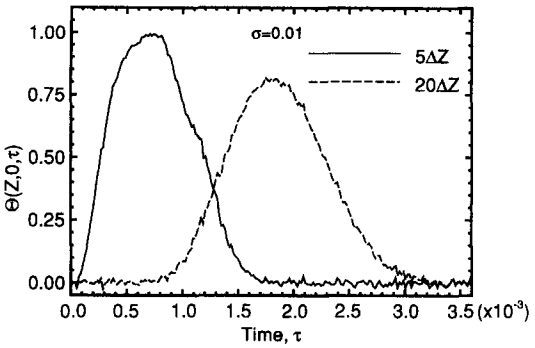

Fig. 6. Simulated measured temperatures at downstream locations $5\Delta Z$ and $20\Delta Z$ for double step pulse, with $\sigma = 0.01$.

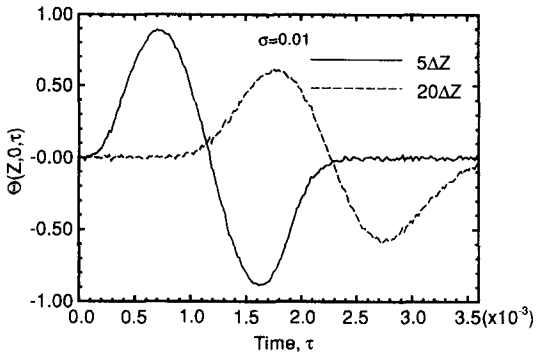

Fig. 8. Simulated measured temperatures at downstream locations $5\Delta Z$ and $20\Delta Z$ for sine curve pulse, with $\sigma = 0.01$.

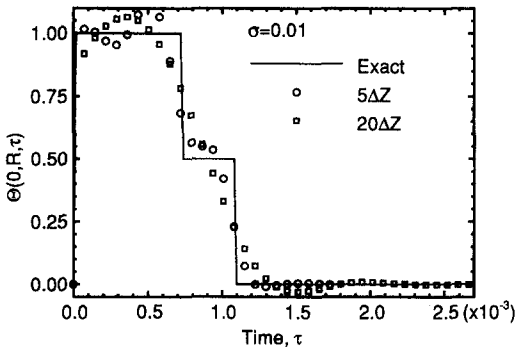

Fig. 7. The effects of sensor locations $5\Delta Z$ and $20\Delta Z$ on the accuracy of the estimate for double step pulse, with $\sigma = 0.01$.

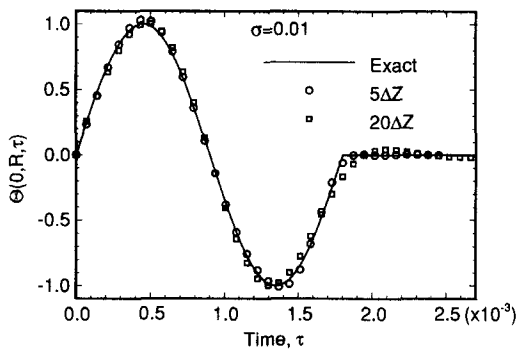

Fig. 9. The effects of sensor locations $5\Delta Z$ and $20\Delta Z$ on the accuracy of the estimate for a sine curve pulse, with $\sigma = 0.01$.

locations. For the $5\Delta Z$ location, the inverse solution tends to follow the discontinuities, including the second step; however, the solution oscillates after the first jump. The results from the $20\Delta Z$ location follow the pulse, but cannot predict the sharp corners at all.

Test case 3: *sine curve*

The inlet condition for the sine curve illustrated in Fig. 2c is assumed in the form

$$F(\tau) = \begin{cases} \sin(1111.11\pi\tau) & \text{for } 0 < \tau \leqslant 1.8\times10^{-3} \\ 0 & \text{for } 1.8\times10^{-3} < \tau \leqslant \tau_f \end{cases} \quad (19)$$

The measured values for this test are represented in Fig. 8. Since the function is smooth over the whole time domain, the inverse analysis is quite accurate for both locations $5\Delta Z$ and $20\Delta Z$, as apparent from Fig. 9.

The effect of the sampling frequency on the accuracy of estimations was also tested. Very high sampling rates (i.e. five times the value used in Figs. 3, 6, 8) produced generally the same results but with slightly more oscillations around the discontinuities and a much large computational time. A smaller sampling rate produced nearly identical results; however, an exceedingly large time step should not be chosen since the inverse problem would then not be able to resolve any change in the function that did not have a large enough period to allow for more than a few time readings.

A CRAY Y-MP super computer was used for all computations, with CPU times ranging from 5 s for the triangular ramp function at $\sigma = 0.03$ to 24 s for the sine curve at $\sigma = 0.01$. The smaller values of σ required more CPU time since a more strict convergence criterion is required by equation (15).

The conjugate gradient method appears to be very effective in estimating the functional form of the unknown timewise variations of the inlet temperature for laminar flow inside a duct.

REFERENCES

1. C. H. Huang and M. N. Özisik, Inverse problem of determining unknown wall heat flux in laminar flow through a parallel plate duct, *Numer. Heat Transfer, Pt A* **21**, 101–116 (1992).
2. R. Raghumath, Determining entrance conditions from downstream measurements, *Int. Comm. Heat Mass Transfer* **20**, 173–183 (1993).
3. A. Moutsoglou, An inverse convection problem, *J. Heat Transfer* **111**, 37–43 (1989).
4. O. M. Alifonov, Solution of an inverse problem of heat conduction by iteration methods, *J. Engng Phys.* **26**(4), 471–476 (1974).
5. Y. Jarny, M. N. Özisik and J. P. Bardon, A general

optimization method using adjoint equation for solving multidimensional inverse heat conduction, *Int. J. Heat Mass Transfer* **34**, 2911–2919 (1991).
6. O. M. Alifonov, Application of the regularization principle to the formulation of approximate solution of inverse heat conduction problem, *J. Engng Phys.* **23**(6), 1566–1571 (1972).
7. IMSL Library Edition 10.0, *User's Manual*, Math/Library Version 1.0. IMSL, Houston, TX (1987).